Coloured poly(vinyl chloride) (PVC) by femtosecond laser machining

K. M. Tanvir Ahmmed,[†] Roozbeh Mafi,[‡] and Anne-Marie Kietzig[*,†]*

[†]Department of Chemical Engineering, McGill University, Montreal, QC, H3A 0C5, Canada

[‡]Canadian General-Tower Limited, Cambridge, ON, N1R 5T6, Canada

KEYWORDS. Poly(vinyl chloride), PVC, colour, femtosecond laser, ablation threshold

ABSTRACT. In this study, we fabricated coloured poly(vinyl chloride) (PVC) by direct femtosecond laser micromachining at infrared (IR) wavelength without the addition of chemical colourants, eliminating the concern of leaching dyes and pigments. Yellow, brown, and black colours were observed on the irradiated samples. A quantitative analysis of the colours, according to the International Commission on Illumination (CIE) standards, was performed to distinguish different shades of these three colours. We determined that the changes in surface chemistry and surface topography both contribute to the colour formation. X-ray photoelectron spectroscopy (XPS) on the machined samples showed that conjugated double bonds are liable for the yellow and brown colour, whereas the presence of oxidized carbon and surface topography contribute to the black colour. Fourier Transform Infrared Spectroscopy (FTIR) indicated that laser irradiation altered the material's properties only near the surface which left the bulk properties unaltered. Furthermore, chemical resistance test showed that some of the coloured PVC were able to

withstand the influence of aggressive chemicals and their colour did not fade. Finally, we showed that the fabrication of coloured PVC highly depends on its ablation energy threshold which is affected by the laser pulse duration and wavelength.

1. INTRODUCTION

Human eyes perceive reflected wavelengths of light from an object as colours. Most colours around us arise from the fact that some wavelengths of light are absorbed by an object with the remainder being reflected to our eyes. Specifically, dyes and pigments in an object contain certain chemical bonds, ions, and radicals that can absorb specific wavelengths of lights. Thus, a dye or pigment is typically used as an additive to provide colour to an object. However, added dyes and pigments that are not bound to the base material can leach out from objects in the presence of a solvent, and the end-of-life disposal of some of these coloured materials is detrimental to the environment because they contain non-bound heavy-metals and free aromatic amines [1]. In addition, the production of these dyes and pigments poses health and safety issues. Structural colours have been presented as a sustainable alternative to pigments and dyes, where colours originate from the interference and diffraction of light by nanostructures that decorate the surface. However, such nanostructures are difficult to manufacture, especially on polymers [2]. Production of coloured polymers without the addition of chemicals or alteration of surface nanostructures can be achieved through degradation processes [3]. This degradation can be due to exposure to high temperatures (thermal degradation), high mechanical stress, and ultraviolet (UV) light. However, the colour change due to these processes are not limited to the sample surface; consequently, these processes affect the bulk properties of the polymer.

In this study, we propose to fabricate coloured poly(vinyl chloride) (PVC) by femtosecond (fs) laser irradiation to overcome the problems with current methods of colour production. Fs laser

micromachining has emerged as a new technique to incorporate new or improve existing properties in different materials [4]. It is a contactless technique that can be used to machine both opaque and transparent materials [5-6]. Furthermore, this method can create microscale and nanoscale surface features in an easy one-step process. Fs laser micromachining has focused primarily on the tuning of surface properties such as wettability and adhesion [7]. However, most surface property alterations are accompanied by a change in colour. The colour change induced by fs laser machining has been studied extensively for metal substrates [8-9]. In contrast, the investigation into the alteration of colour in laser irradiated polymers is scarce [10-11]. Most studies on fs laser micromachining of polymers have focused on surface feature formation [7]. Nevertheless, in several applications, the visual appearance of the machined sample is as important as its other enhanced properties [10]. Laser ablation brings about both chemical and structural changes which alter the optical properties of the machined part. Thus, the colour change is a direct consequence of many surface property modifications. Yet, changing the colour of an object can be useful even without other surface property modifications [10, 12].

Laser-induced colour changes happen only to the precise location of the sample surface that is irradiated with the laser beam. Therefore, this technique can be used for generating colours at selected positions of a sample. Further, as femtosecond pulses are extremely short and the ablation mechanism is fundamentally different from long pulse (ns and longer) laser beams, the heat affected zone is very small [13]. Thus, only the surface properties of the materials are affected, preserving the integrity of the bulk.

To exploit the benefits of laser-induced colour formation on polymers, we took the first step to investigate the range of colours that can be generated on poly (vinyl chloride) (PVC). The choice of the polymer was made because of its widespread use. PVC is the third most used polymer in

the world with 12% of the world's polymer production [14]. Moreover, PVC with different colours is in demand for different products, e.g. imitation leather. Previous laser ablation studies of other polymers showed that laser parameters, such as pulse duration and wavelength, influence structural and chemical change [15-16]. The interaction of PVC with the fs-laser beam leading to structural and chemical change is a completely unstudied topic. Thus, an investigation on the effect of these parameters on PVC ablation is a necessary first step to achieve colour by machining with different laser systems.

2. MATERIALS AND METHODS

2.1 Laser machining. An amplified Ti:Sapphire laser (Libra, Coherent Inc.) was used to micromachine the PVC samples. The laser was operated at a repetition rate (f) of 1 kHz and produced a horizontally polarized Gaussian beam. Type I clear PVC sheets were purchased directly from McMaster-Carr (Catalogue No. 87545K73). The samples were 1.6 mm thick and had a density of 1.4 g/cm^3. The pulse duration of the laser beam was varied from 67 fs to 230 fs. An optical parametric amplifier (OPerA Solo, Coherent, Inc.) was used to modulate the wavelengths of the laser beam from 275 nm to 1400 nm. The power (P) of the laser beam was adjusted by a computer controlled variable attenuator which consists of a half-wave plate and a polarizing beam splitter. The samples were placed on a computer-controlled stage. The stage can move in 3 directions and was operated with a commercial software (Gol3D, GBC&S). While the laser beam was stationary, the stage was moving at a velocity (v) ranging from 0.21 mm/s to 33 mm/s. The laser beam was focused onto the sample by a plano-convex lens having a 100-mm focal length. The beam diameter (ω_0) at focus was measured as 56 μm. Laser machining was conducted in air. A ventilation system next to the machining plane was used to remove the generated by-products

including nanoparticles. The machined samples were placed in a beaker containing ethanol and cleaned ultrasonically for five minutes to remove the loose debris.

Raster scanning was performed to irradiate an area larger than the beam diameter. Thereby, lines etched by the laser beam in the horizontal direction (*x*) were overlapped in the vertical direction (*z)*. Thus, individual line widths at certain machining parameters were measured to calculate the line overlap distance (centre-to-centre distance between two successive lines, Δz). The pulses-per-spot (*PPS*) were calculated from the horizontal and vertical overlap of pulses by the following equation [17]:

$$PPS = (PPS_x)(PPS_z) = \left(\frac{\omega_0 f}{v}\right)\left(\frac{\omega_0}{\Delta z}\right) \quad (1)$$

Energy flux is another machining parameter which was varied by controlling the power of the laser beam. It is expressed as fluence (F), which is defined by the following equation [17]:

$$F = \left(\frac{8P}{\pi {\omega_0}^2 f}\right) \quad (2)$$

The threshold fluence for ablation was determined by linewidth measurements. It was previously established that the diameter (D) of an ablated feature at any fluence is related to the beam diameter (ω_0) and the threshold fluence (F_{th}) by the following equation [18-19]:

$$D^2 = 2{\omega_0}^2 \times \ln\left(\frac{F}{F_{th}}\right) \quad (3)$$

Figure A1 (a) (supporting information) shows the plot used for threshold fluence measurement. Squares of the measured line widths are plotted against the fluence values in logarithmic scale. The x-intercepts of the extrapolated lines give the threshold fluence values. However, these experimental results can only be used for the specified PPS. To find the threshold fluence at any PPS, the incubation model was used [20]:

$$F_{th}(PPS) = F_{th}(1) \times (PPS)^{S-1} \quad (4)$$

where $F_{th}(PPS)$ is the threshold fluence at PPS number of pulses-per-spot, $F_{th}(1)$ is the threshold fluence for a single pulse, and S is the fitting parameter termed as the incubation coefficient. By using the threshold fluence values at four different PPS, we calculated the incubation parameters by using equation 4. The plot for finding the parameters is shown in Figure A1 (b).

2.2 Chemical characterization. The chemical analysis of the samples was conducted by X-ray Photoelectron Spectroscopy (XPS) and Fourier Transform Infrared Spectroscopy (FTIR). XPS measurements were conducted over a 400 μm spot size (K-alpha, Fisher-Scientific). An Argon ion flood gun was turned on during measurements to compensate for surface charging. Both survey scans and high-resolution scans were conducted for all the samples. Survey scans were performed to determine the elemental composition (3 scans at 200 eV pass energy and 10 ms dwell time). A high-resolution scan was conducted for O1s, C1s, and Cl2p to determine the bonding structure (10 scans at 50 eV pass energy and 50 ms dwell time). FTIR was carried out with an instrument having an Attenuated Total Reflection (ATR) accessory attached to it (PerkinElmer Spectrum 100).

2.3 Topographical analysis. Scanning Electron Microscopy (SEM) was used to analyze the surface topography of the irradiated samples. For preliminary test samples, a thin layer of gold was coated on them before imaging with the SEM (FEI Inspect F50). For the final samples which went through optical and chemical analysis, no coating was necessary for imaging in a low-vacuum mode with the environmental SEM (FEI Quanta 450). Single scan line width measurements were conducted with an optical microscope (Leica EZ4 D).

2.4 Optical characterization. The images of the coloured samples were captured under artificial daylight provided by Daylight Macbeth SpectraLight II. The transmission curve for the control PVC sample was generated by a UV-VIS spectrophotometer (Thermo Scientific Evolution 100). All other optical measurements, namely reflectivity and colourimetry, were conducted with a

spectrophotometer having an integrating sphere (Datacolor 600). The spectrometer has a barium-coated integrating sphere. D/8° viewing geometry, D65/10° illuminant, and 6.5 mm aperture were used for all the measurements with the datacolor spectrometer. The spectrometer provided the colourimetric data in CIE L*a*b* coordinates, where L is the lightness of the colour, a and b are the dimensions of the two colour-opponents red/green and yellow/blue, respectively. These colourimetric data are device-independent and can only be plotted on a three-dimensional space.

2.5 Chemical resistance of the colours. We also conducted a chemical resistance test by exposing the machined samples in an aqueous solution of trichloroisocyanuric acid, an oxidizing agent, for 24 hours. The concentration of the chemical in water was 7 ppm. Whether a sample had changed its colour or not was confirmed by measuring the colour difference (ΔE*) of the exposed samples according to the "CIE 1976" standard with the Datacolor spectrometer. Colour difference (ΔE*) is a derived parameter that encompasses the difference in all three components of Lab coordinates. When the ΔE* value were smaller than 1, then we considered that there were no differences in colours between the standards (before exposure to the chemical) and the test samples (after exposure).

3. RESULTS AND DISCUSSION

3.1 Laser machining and optical properties. Ten samples were irradiated using different machining parameters to investigate colour formation. Table 1 shows the line overlap distance (Δz), velocity, and power used to machine each sample. Pulses-per-spot (PPS) and experimental fluence values were calculated from the machining parameters and are also tabulated in Table 1. Threshold fluence values at each PPS were experimentally determined and are shown along with the experimental fluence values. Samples which were irradiated at a fluence lower than the threshold fluence are marked with shades. A non-machined PVC sample was used as a control

sample and is designated as sample S11 in the subsequent discussion. In addition, a 12th sample was machined for the sole purpose of surface texture investigation, which will be discussed later.

Table 1. Machining parameters for each sample along with their pulses-per-spot (PPS) and fluence values.

Sample name	Δz, μm	Velocity, mm/s	PPS	Power, mW	Threshold Fluence, J/cm^2	Fluence, J/cm^2
S1	2.5	2.1	711	3.8	0.4	0.26
S2	2.5	2.1	711	10.5	0.4	0.72
S3	2.5	2.1	711	16.3	0.4	1.11
S4	2.5	2.1	711	36	0.4	2.45
S5	6	4.2	148	5.8	0.64	0.40
S6	6	4.2	148	12.6	0.64	0.86
S7	6	4.2	148	20.5	0.64	1.39
S8	6	2.1	296	7	0.52	0.48
S9	6	0.21	2964	7	0.27	0.48
S10	6	0.21	7115	3.8	0.21	0.26
S11	Control sample without laser irradiation					
S12	6	0.21	7115	4.3	0.21	0.29

The PVC samples used in our experiments are transparent and lack any discernible colour, whereas the machined samples showed discernible colours in the visible range. Figure 1 shows the coloured samples under daylight illumination plotted on a semi-log graph of fluence versus PPS according to their respective machining parameters. Samples with light yellow colours were irradiated with fluence values below the threshold fluence. Generally, at low PPS, the machined

samples are yellow-brownish in colour. With increasing PPS, the resulting colour turns darker and reaches black at high PPS.

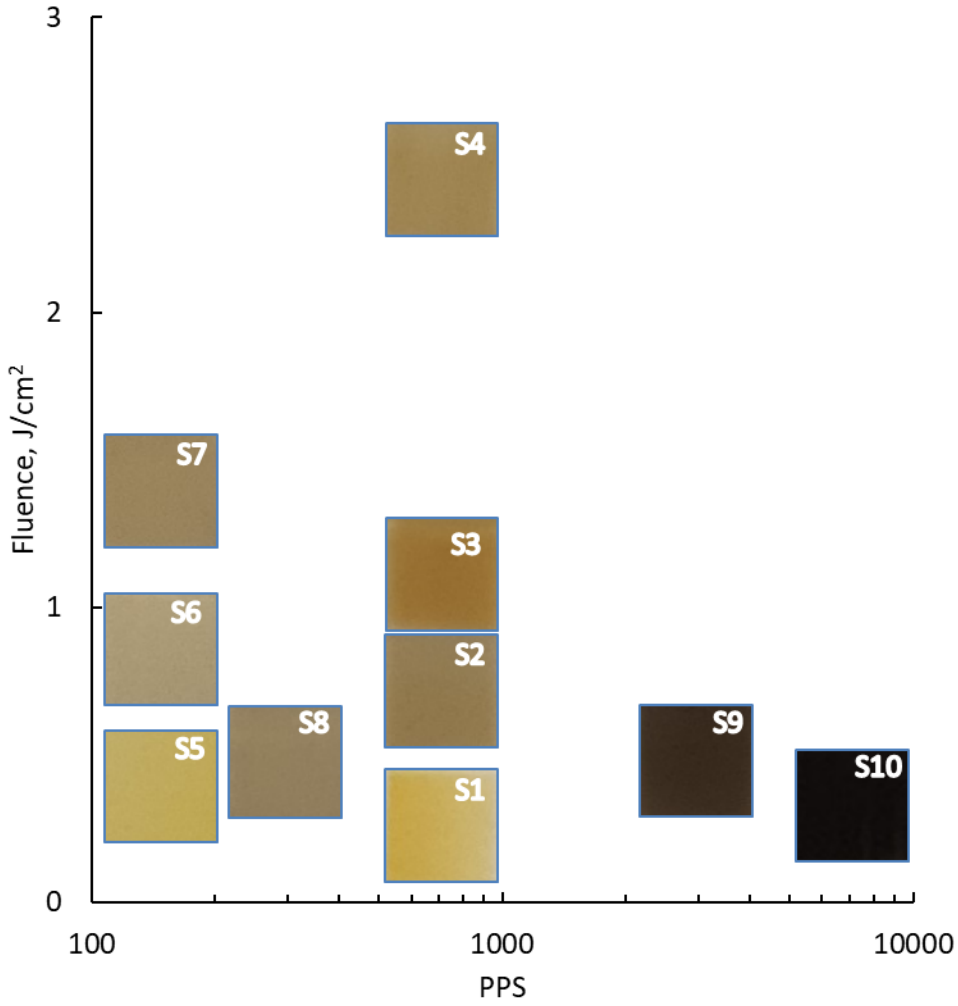

Figure 1. Coloured PVC samples plotted on a semi-log graph of fluence versus pulses-per-spot (PPS).

For comparison purposes, we further quantified the colours seen in Figure 1. The colourimetric data were acquired by spectrometry in CIE L*a*b* coordinates. However, to plot these data on a 2D colour space (chromaticity diagram), we first converted the L*a*b* values into XYZ coordinates according to the "CIE 1931" standards, and eventually transformed the XYZ coordinates into xy coordinates. Figure 2 displays our samples' colours on the chromaticity

diagram using these two derived parameters, x and y. It is to note that the black (sample S10) and the transparent control sample (sample S11) are located very close to each other on the plot, as their respective chromaticity is similar; yet, their brightness is different, which cannot be shown on this 2D chromaticity plot.

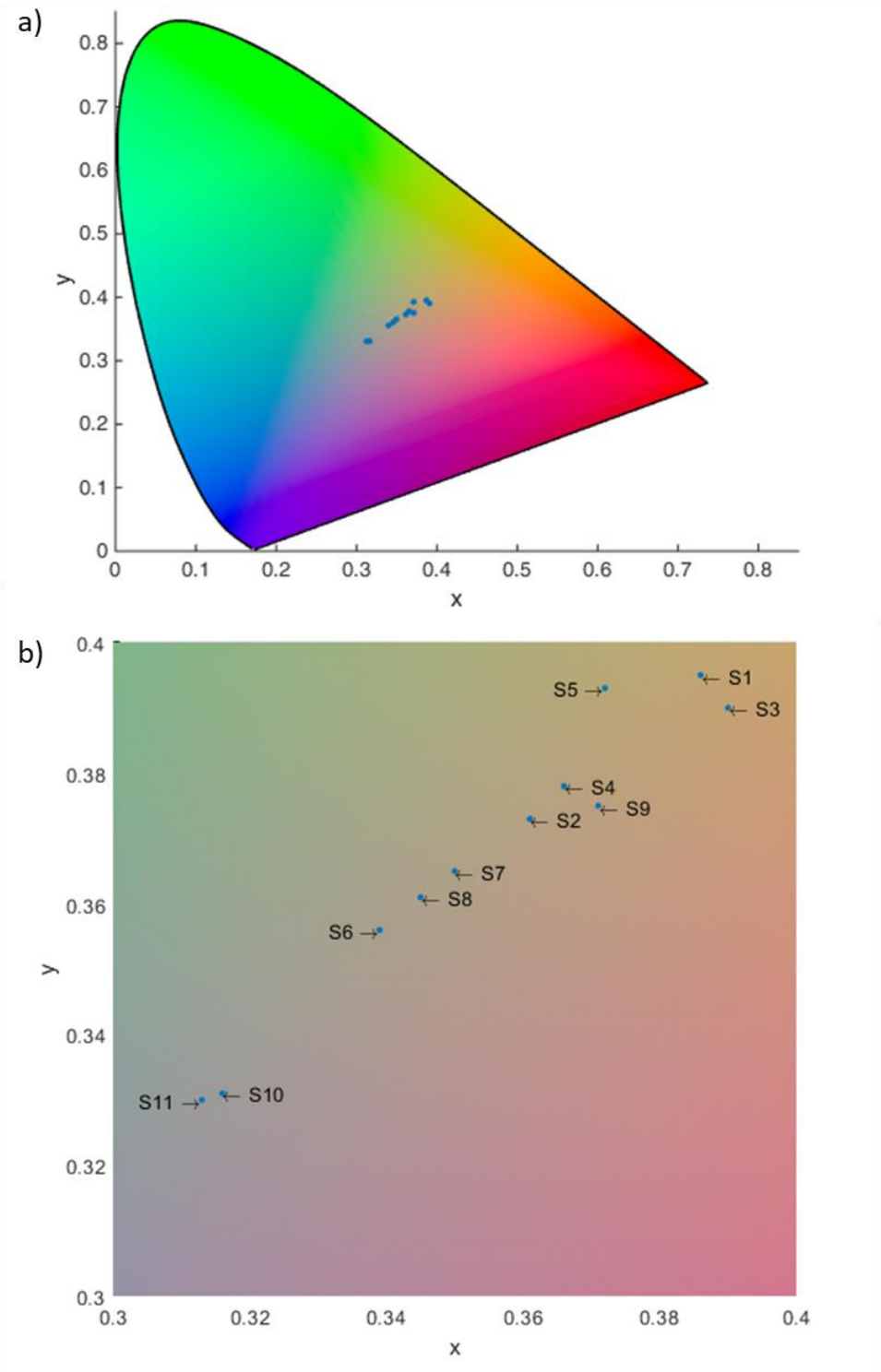

Figure 2. (a) The chromaticity values of the samples are plotted on a CIE 1931 colour space. (b) A magnified view of the same plot.

In addition to the quantification of the samples' colours, we measured the reflectivity of them, and the values are compared in Figure 3. The two dark samples (sample S9 and S10), which were machined at high PPS, have the lowest reflectivity among all the samples. Most of the visible light is absorbed on these two samples, and thus they are no longer transparent after machining. On the contrary, samples machined at low PPS and low fluence (sample S1 and S5) have a similar reflectivity as the non-machined sample (sample S11). All other samples have a higher reflectivity at most of the wavelengths in the visible range. Finally, the absorbance of the samples was also measured and the plot of the absorbance for all the samples is shown in Figure A2 of the supporting information.

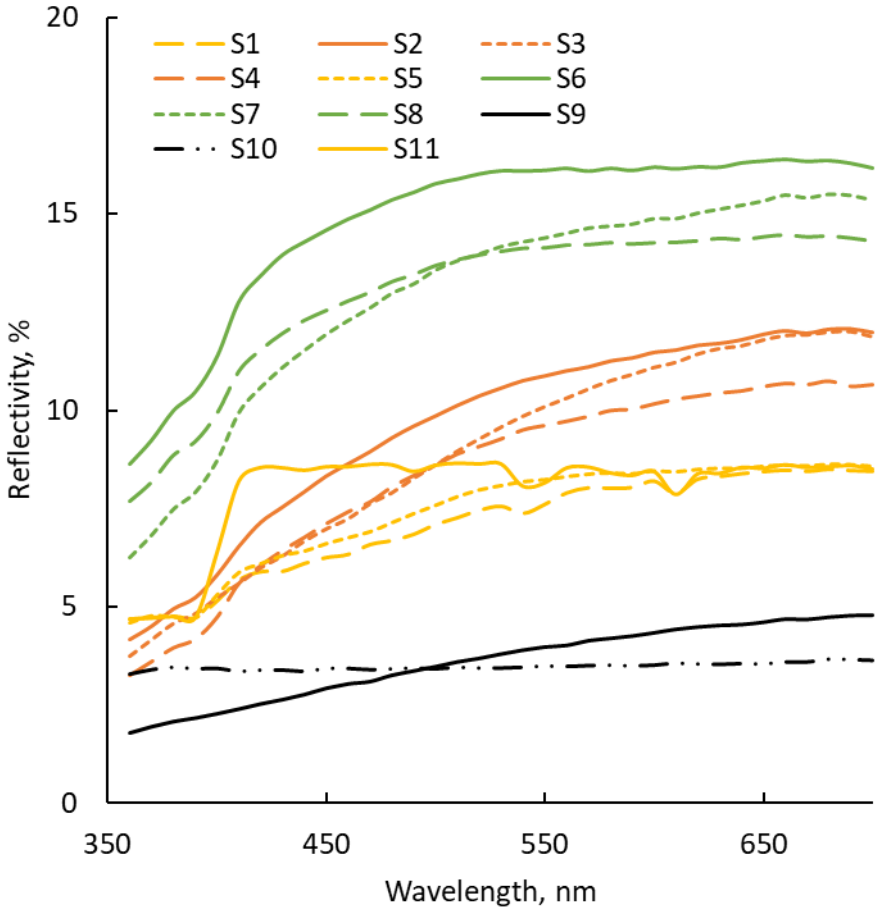

Figure 3. The reflectivity of the samples is plotted against the wavelengths of visible light.

3.2 Surface topography. To understand the origin of the colours, we first conducted a topographical analysis of the machined samples. Figure 4 shows the SEM images of the machined samples. From these SEM images, we observe that all the samples (Figure 4(a)—4(h)) except sample S1, S5, and S8 went through a topographical change. Sample S1, S5, and S8 have no observable change on the surface (Figure 4 (i) and Figure A3 in the supporting information). It is to note that these three samples were machined below ablation threshold fluence. However, even though no ablation occurred, these samples still exhibit colour. Other samples have different surface topographies depending on their machining parameters. When machined at 711 PPS, a sample with low fluence showed a network of filamentous structures (Figure 4 (a)). With increasing fluence, these structures agglomerated (Figure 4 (b)) and eventually formed nodular structures (Figure 4 (c)). At a low PPS of 148, sample S6 exhibited a different topography. This sample has a perforated texture without any sign of filamentous structure (Figure 4(d)). However, with increasing fluence, the sample surface turned into a network of filamentous structures (Figure 4(e)). In summary, the evolution of the topographical change at low PPS can be described as follows: at the lowest fluence which was below the threshold, there was no structural change, with increasing fluence structures appeared, and with even higher fluence the structures started to agglomerate.

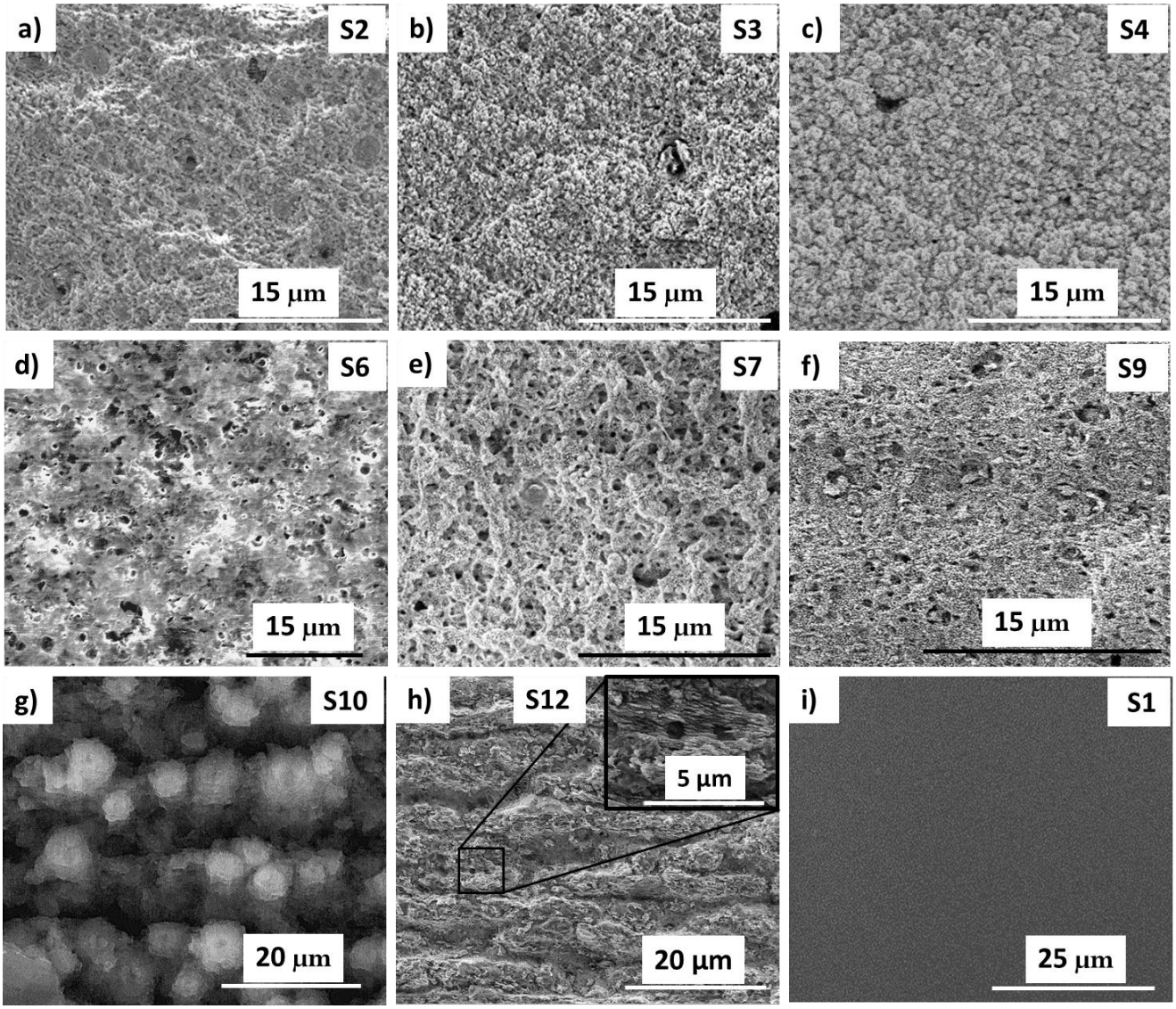

Figure 4. SEM images of the machined samples. a) sample S2, b) sample S3, c) sample S4, d) sample S6, e) sample S7, f) Sample S9, g) sample S10, h) sample S12 and i) sample S1. Sample S5, sample S8 and sample S11 are similar to sample S1, lacking any feature (Figure A3 in the supporting information).

The surface textures at high PPS are shown in Figure 4 (f), (g), and (h). These three samples are darker compared to the other samples. At low fluence, sample S9 exhibits the filamentous structures (Figure 4 (f)). However, this network of filaments appears to be more porous than the

texture observed on the samples machined at low PPS and low fluence (Figure 4(a) and (b)). In contrast, sample S10 exhibits a completely different texture on the surface. This sample has a pillar-like structure, where the pillars have visible nano-textures on them.

Finally, to further investigate the structure formation on sample S10 (Figure 4(g)) which was machined at the highest PPS of 7115, we fabricated another sample where we kept the same PPS but increased the fluence to 0.29 Jcm^{-2} (sample S12). Figure 4(h) shows the texture of this sample. At this high fluence, the pillars are merged together, and a ripple-like structure decorates the elongated pillars. These ripple-like structures are defined as Laser Induced Periodic Surface Structures (LIPSS), and they have a periodicity close to the wavelength of the laser beam [4]. To the best of our knowledge, this is the first report of Laser Induced Periodic Surface Structures (LIPSS) formation on PVC with a femtosecond laser. Like the pillar-covered sample, this ripple-decorated sample is black in colour.

The formation of different surface structures observed on our laser-irradiated polymer samples can be explained by a combination of several mechanisms proposed by other researchers [6]. Both thermal and non-thermal effects are considered to have an effect on the final surface morphologies. The formation mechanism of LIPSS is well established as this morphology is also observed in metals and semiconductors. The LIPSS, as observed on sample S12, forms due to the interference between the incident laser pulses and scattered waves at the surface of the polymer [21]. The filamentous structure is attributed to the bubble formation during melt-resolidification of the PVC polymer [22-23]. The perforated structure is formed just above the ablation threshold of the polymer due to explosive boiling and spallation [22]. These structures eventually lead to the filamentous structures either by increasing the number of pulses or fluence delivered on the sample.

3.3 Chemical analysis. After studying the topographical change of the coloured samples, we investigated their chemical changes. We performed an FTIR spectrum analysis on the as-received vinyl sheets to identify the compounds present. Figure 5 shows the resulting FTIR spectrum along with the characteristic absorption peaks of PVC. In this spectrum, the peak at 2919 cm^{-1} corresponds to a C-H stretch bond, whereas the peaks at 1427 cm^{-1} and 1250 cm^{-1} correspond to C-H bending bonds. Finally, the characteristic absorption peaks for PVC are identified at 963 cm^{-1} as the C-C stretch bond and at 690 cm^{-1} as the C-Cl stretch bond [24]. They correspond to the PVC backbone chain and the Cl attached to it, respectively. This FTIR spectrum confirms that the sample material used is indeed PVC without any noticeable additives.

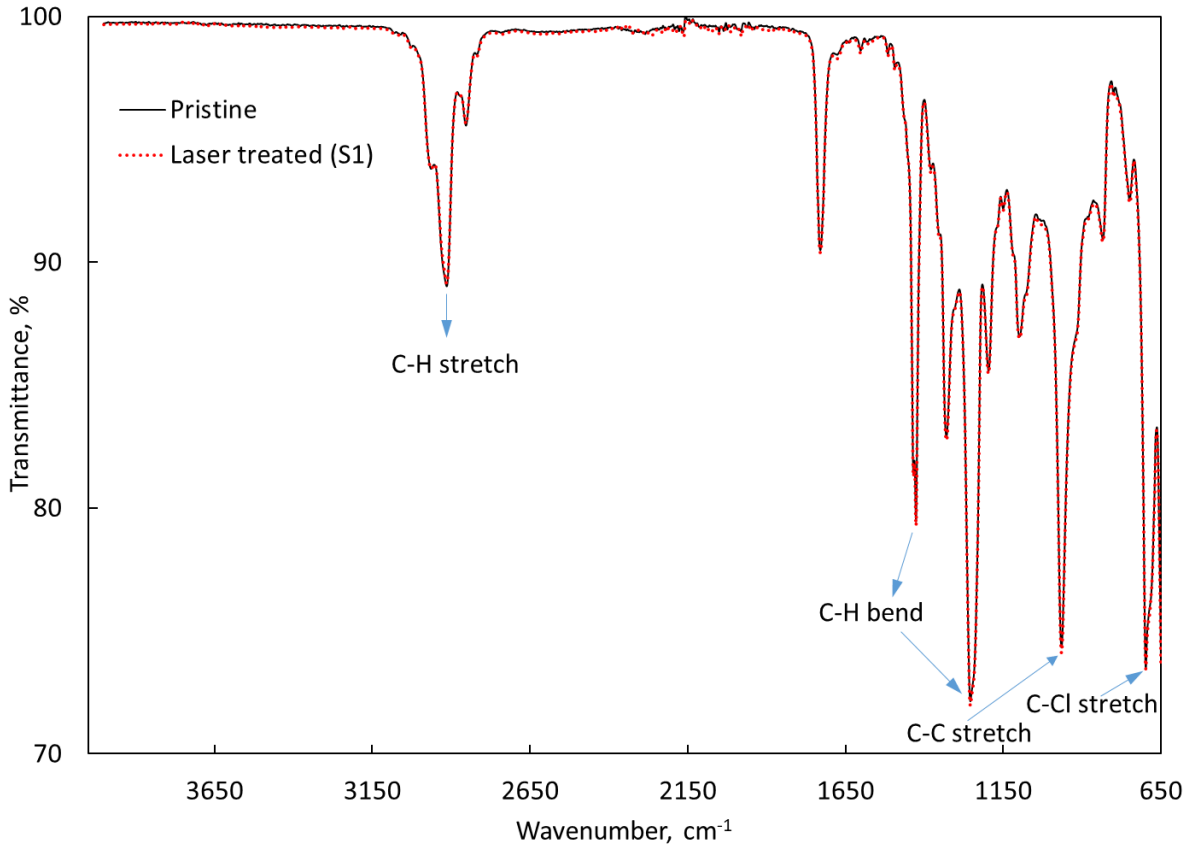

Figure 5. FTIR spectrum of the as-received vinyl sheets and the laser irradiated sample S1. The characteristic absorption peaks of PVC (at 963 cm^{-1} and 690 cm^{-1}) are identified and labelled on the spectra.

We also performed the FTIR spectra analysis on irradiated samples with no visible structural change. Surprisingly, the spectrum of these samples and the spectrum of the non-machined sample are the same (Figure 5 and Figure A4 of the Supporting Information). We did not conduct the FTIR analysis on the rest of the irradiated samples where the surface topography did change in order to avoid the destruction of the micro/nanostructures of the sample surface. As an alternative, we used XPS to probe the change in surface chemistry for all the irradiated samples. However, the FTIR results on the non-ablated irradiated samples were still used for comparative purposes.

Figure 6 shows the elemental composition of all samples. According to the XPS analysis, all the machined samples went through a chemical change. The non-machined sample (sample S11) shows the presence of oxygen that after argon sputter cleaning reduces to ~1% from the initial content of ~3%. The oxygen content of the machined samples is higher than that of a non-machined sample, whereas the Cl content is lower. On the other hand, the carbon content in samples S1 and S5 is similar to that of a non-machined sample. Moreover, these two samples have higher Cl content compared to the other machined samples.

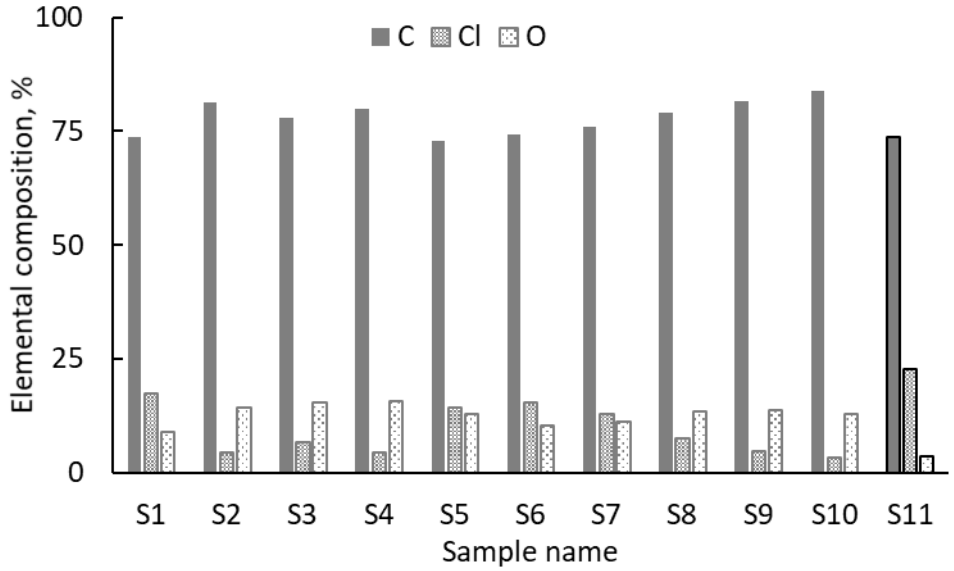

Figure 6. Elemental composition of the samples obtained by XPS analysis. The analysis was conducted on a spot size of 400 µm located at the centre of a 500 µm square sample.

High-resolution XPS spectra of the samples also confirmed the presence of oxides on them. Figure 7 shows the spectra of the machined samples. Peaks at 285.9 eV and 287 eV are representative of C-C (also C=C) and C-Cl structures. It is to note that even the control sample had a low amount of oxides at 288.9 eV (Figure 7(a)). This peak indicates the presence of a small amount of impurities on the surface of the PVC sample. However, after machining, the oxygen content increased to 2.5—4.3 times the original value. No new chemical structure was noticed on

sample S1 (Figure 7(b)), which was irradiated below threshold fluence. Sample S5 showed similar result as sample S1 (Figure A5 (a) in the supplementary information). However, sample S8 was machined below threshold fluence but it showed a new chemical structure, the O-C=O bond (Figure 7(c)) at 289.9 eV, this phenomenon can be attributed to the sample being machined very close to the threshold fluence. On samples machined at a fluence beyond the threshold fluence, O-C=O bonds were also detected (Figure 7(d)). For the samples machined at 711 PPS, at high fluence (>1 J/cm^2), i.e. sample S3 and S4, a detectable amount of conjugated C=C bonds were identified as small peaks located at 292—293 eV (Figure 7(e) and (f)). These small peaks, located at 6—7 eV higher than the main C1s peak's binding energy, are called satellites. They indicate the presence of unsaturation, specifically conjugated double bonds, in the polymer chain [25]. A satellite was also identified on sample S9 machined at high PPS and low fluence (Figure 7(g)). However, satellites were not detected on the black sample which was machined at the highest PPS (Figure 7(h)). In conclusion, at low PPS, when machined below threshold fluence there was no new detectable chemical structure, whereas with increasing fluence new structures such as C=O and O-C=O were observed; at even higher fluence satellite peaks marking the presence of conjugated bonds were detected. However, at moderately high PPS, satellites were detected at low fluence which then disappeared at very high PPS.

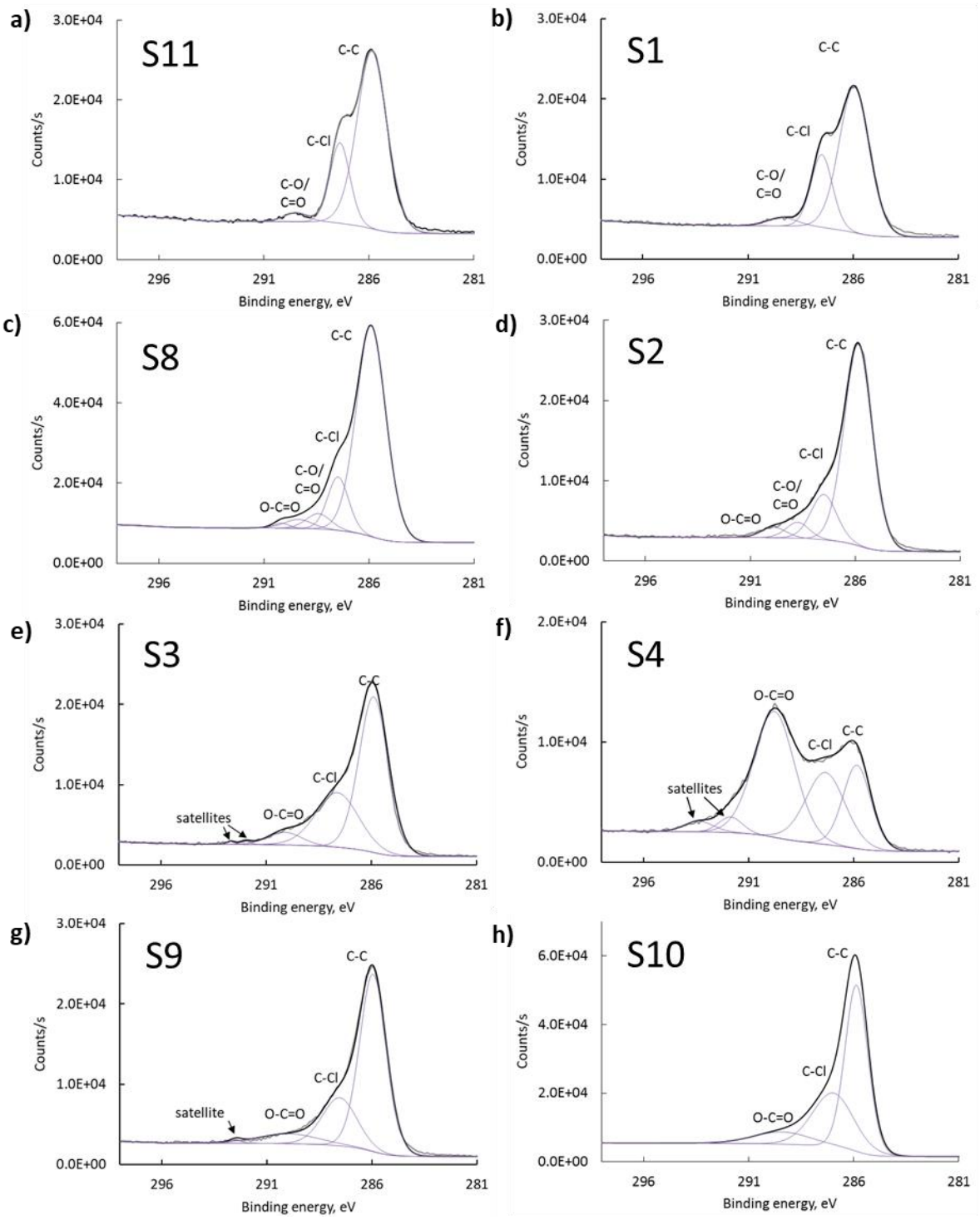

Figure 7. High-resolution XPS of C1s of a) control sample S11, b) sample S1, c) sample S8, d) sample S2, e) sample S3, f) sample S4, g) sample S9, and h) sample S10. Sample S5 has a similar

profile as sample S1, whereas sample S6 and S7 has a similar profile as sample S2 (Figure A5 in the supporting information).

3.4 Origin of the colour change. Based on our results presented earlier, it is evident that to determine the reason behind the colour change a discussion is required that encompasses both optical properties as well as structural and chemical change. In Figure 3, we observed that the reflectivity of sample S1 and S5 were similar to the reflectivity of the control PVC sample (S11). This similarity in reflectivity suggests that these samples went through minimal or no chemical and/or structural change. Furthermore, in the SEM images of Figure 4, we found that these irradiated samples have no observable surface texture, and they resemble the control sample. However, even without any modification of the surface texture, these samples show colours in the visible range. Therefore, we conclude that the colour on these samples results only from chemical changes induced by laser-material interaction. However, the FTIR analysis did not show any change in surface chemistry. This unexpected result can be explained by the nature of the FTIR measurement method. Usually, FTIR probes 0.1 to 2 µm deep into the sample. Whereas, the femtosecond laser-material interaction occurs at the topmost surface [26]. Thus, if there is any chemical change in the first few nanometers of the sample, the FTIR probe is not suitable to detect it, whereas XPS gathers data from the top 5-10 nm of a surface. The elemental analysis from XPS measurements confirms that these two samples indeed went through chemical change as the amounts of C and O present in these samples are higher than the control sample. However, high-resolution XPS did not reveal any new chemical bonds. We hypothesize that these two samples, S1 and S5, went through the least amount of chemical change among all the irradiated samples because they were machined below the threshold fluence values. We based our hypothesis by considering the laser-matter interaction. At infrared wavelength, the only way to absorb laser

energy and undergo chemical reaction is to initiate non-linear absorption [13]. However, a minimum pulse energy is required to initiate non-linear absorption. Therefore, any chemical or physical change can only occur if the pulse energy (thus the fluence) is higher than a threshold pulse energy (thus the ablation threshold fluence). However, below threshold fluence localised change can still occur due to the inhomogeneity of the surface as properties of the material, including defects and roughness, can affect this minimum threshold fluence [6].

All the other irradiated samples have a different reflectivity than the control sample. They also have a different surface texture compared to the control sample which indicates that these samples went through a significant structural change. Furthermore, the elemental compositions of all these samples are different from the control, indicating a chemical change. In addition, the high-resolution XPS analysis shows new chemical bonds present in these samples. Therefore, we conclude that both the chemistry and structure affected the optical properties of these samples.

Yellow colours similar to our machined samples' colours were previously observed on PMMA after ultrafast laser machining [10]. The yellow colour on PMMA was attributed to the conjugated C=C bonds without providing any chemical analysis. However, another study by Blazevska-Gilev, et al. confirmed the presence of conjugated C=C bonds on deposits ablated from PVC with an IR laser (ns pulses) [27]. FTIR and Raman spectroscopy were used to confirm the conjugated bonds. Blazevska-Gilev's study did not mention any coloured sample and the presence of conjugated bonds were reported on the laser ablated deposits (ejected from the target sample) rather than the target sample. However, we hypothesize that the same conjugated bonds are present in our target sample. The high-resolution XPS data of C1s of three of our samples confirmed the presence of these conjugated double bonds (Figure 7 (e), (f), and (g)). These samples were irradiated at high PPS (≥711) and fluence ($>F_{th}$) compared to the other samples. The only exception is sample S10,

which was irradiated at the highest PPS of 7115. At this high PPS, the initially formed polyenes could be completely ablated and/or polymerized so that C=C bonds disappear. For all the other samples the concentration of the conjugated double bonds was below the detection limit of our current measurement method. We also note that Blazevska-Gilev's study could not detect the conjugation bond from the high-resolution XPS data, rather Raman spectroscopy on the debris was performed to detect the polyenes [27].

It is well known that polymers form polyenes (compounds with conjugated double bonds) during thermal, photochemical and chemical degradation [28]. However, the formation of conjugated bonds during laser ablation is fundamentally different from other degradation methods, namely thermal and UV [29]. At first, the PVC sample undergoes a homolytic scission during the exposure of the IR laser beam (Figure 8). Unlike the thermal decomposition, during fs laser machining the monomer breaks away from the main polymer backbone, and vinyl chloride gas is released [27, 30]. On the other hand, homolysis of two distant C-C bond results in two diradicals which leads to the evolution of HCl gas and C=C bond. A single C=C does not absorb light in the visible range. However, ultrafast laser ablation can propagate the decomposition and produce conjugated bonds. These conjugated bonds can absorb light in the visible range. With increasing chain length of the conjugated bonds, the observable colour shifts towards the yellow-orange region. The ablated PVC deposits in the previous study had polyene chain length of 13 [27]. Thus, we conclude that the yellow colour of the machined samples is because of the conjugated C=C bonds.

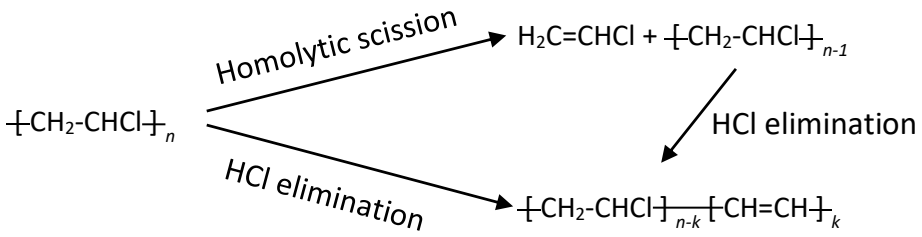

Figure 8. Conjugation bond formation scheme [27].

We can also explain the lightness (L*), the perceived brightness of colour, of the machined samples by considering the carbon (C) content of the samples and the strength of the satellite peaks (Table 2). In the CIE Lab standard, L*=100 represents the brightest white, whereas L*=0 represents the darkest black. A sample with high C content is darker than a sample with low C content. Similarly, the darker colours are due to the prominent presence of the satellite peaks in the XPS spectra. The colour of the samples was also affected by the surface topography. Samples with multiple length scale structures are efficient in absorbing light. Thus, sample S10 is dark in colour with the lowest reflectivity.

3.5 Chemical resistance. We also conducted a chemical resistance test to investigate the stability of the produced colours. The colour difference (ΔE*) of the samples before and after exposing them to an aqueous solution of trichloroisocyanuric acid are listed in Table 2, along with the individual component of the colourimetric data (L*a*b*) before exposure.

Table 2. Lightness (L*) and colour components (a* and b*) of the samples along with their carbon content. The last column shows the colour difference after exposing the samples to an oxidizing agent.

Sample #	C content, %	L*	a*	b*	ΔE*
S1	73.7	80.99	3.78	33.6	1.13
S2	81.3	52.68	1.88	15.67	2.37
S3	78.0	50.45	5.09	22.51	2.45
S4	80.0	54.64	1.97	17.86	3.10
S5	72.9	84.71	-0.56	31.32	0.26
S6	74.3	62.45	0.17	10.51	0.73
S7	76.0	59.03	1.03	13.51	1.63
S8	79.0	59.37	0.48	12.08	0.70
S9	81.7	30.25	2.81	11.61	2.66
S10	83.8	22.00	0.29	0.36	0.74
S11	73.6	90.65	-0.10	0.32	0.41

This chemical resistance test showed that, among the ten irradiated samples, sample S5, S6, S8, and S10 passed the test (ΔE* values < 1 are marked with shades in Table 2) which means that their colour did not fade even after exposure to the oxidizing agent. The reason for the colour change of other irradiated samples can be the disappearance of some of the conjugated bonds that are responsible for the colours. The transformation of the conjugated bonds due to the polymerization of the C=C bonds is noted in another study [27]. We cannot be certain as for why the polymerization happened only on some of the samples. However, we hypothesize that a high density of conjugated bonds on the surface may facilitate the polymerization, as in the case of samples S3, S4, and S9. This disappearance of conjugated bonds can happen even without the presence of chemicals. Thus,

the results are not conclusive as for whether the colour change is due to the oxidizing agent or not. Even though only 4 samples showed stability in colour, the result is still promising as we can make stable yellow, brown and black colours on PVC without modifying the bulk properties of the material or without adding any chemicals. As there is no addition of pigments and dyes in our laser-irradiated coloured samples, there is no issue of dye leaching and no end-of-use disposal problem. Thus, producing the coloured samples by laser machining can be considered a greener approach. While this study introduced laser machining as a green alternative for fabricating coloured PVC, additional research must be conducted to verify the suitability of the coloured PVC in potential applications as the thermal stability of the polymer might be affected by laser machining.

3.6 Threshold fluence of PVC. Finally, it is clear from our results that sample colour highly depends on fluence and PPS. In addition, laser irradiation above or below the threshold fluence results in different surface textures. However, this ablation threshold of polymers highly depends on the number of laser pulses (PPS) deposited on the samples [23]. A laser beam with different beam properties than ours will have a different threshold fluence for PVC even at a PPS similar to our work. Thus, we investigated the effect of different wavelengths and pulse durations on threshold fluence. PVC samples were irradiated at three different pulse durations and three different wavelengths. By measuring the widths of the lines fabricated in these experiments, we calculated the incubation coefficient and single pulse threshold fluence according to the procedure described in the methods section. The values are tabulated in Table 3.

Table 3. Single-pulse threshold fluence and incubation coefficient for PVC at different laser parameters.

Laser parameters →	67 fs, 800 nm	130 fs, 800 nm	230 fs, 800 nm	130 fs, 400 nm	130 fs, 275 nm
$F_{th}(1)$	1.55±0.09	2.71±0.19	8.06±0.81	1.20±0.07	0.73±0.04
S	0.84±0.01	0.71±0.02	0.58±0.03	0.61±0.02	0.59±0.02

According to the result presented in Table 3, the threshold fluence for a single pulse increases with increasing pulse duration as shorter pulses have higher temporal energy density. Similarly, the single pulse threshold fluence increases with increasing wavelength as short wavelengths have higher power compared to longer ones. By using these tabulated values, the machining parameters to create colour on PVC samples can be estimated for a wide range of laser beams with different pulse durations and wavelengths. However, we also note that machining at wavelengths below the cut-off wavelength (389 nm) of PVC might show different colours than the ones depicted in Figure 1 as the absorption of light is high in UV regime for PVC (Figure A6 of the Supporting Information).

4. CONCLUSION

Coloured PVC samples were created by femtosecond laser irradiation without adding any dyes or pigments. The resulting colours were quantitatively analyzed using the CIE standards. We found that both the surface chemistry and surface topography contribute to the resulting colour. However, SEM analysis showed that colour could be obtained even below ablation threshold fluence without any visible change in surface topography. In this case, the colour is purely due to the change in surface chemistry. Chemical analysis of the irradiated samples showed the presence of conjugated double bonds. These conjugated double bonds are responsible for yellow and brown colours,

whereas a high level of carbon and multiscale roughness rendered the sample black. As both the structural and chemical change depend on the laser parameters such as pulse duration and wavelength, we investigated their effects on ablation threshold of PVC. Therefore, the results from our study will guide coloured PVC production by different fs laser systems. Finally, the chemical resistance test showed that some of our coloured samples did not fade even in the presence of an oxidizing chemical. Thus, our work introduces laser machining as a green solution to produce certain stable colours without adding any chemicals.

AUTHOR INFORMATION

Corresponding Author

* Tel: +1(514) 398-3302. E-mail: anne.kietzig@mcgill.ca

Author Contributions

Dr. K. M. Tanvir Ahmmed wrote the manuscript, designed and conducted all the experiments, and all the analyses. Dr. Roozbeh Mafi supervised the work and edited the manuscript. Prof. Anne-Marie Kietzig supervised the work and edited the manuscript.

Notes

The authors declare no competing financial interest.

ACKNOWLEDGEMENT.

This research was jointly funded by MITACS and Canadian General-Tower Limited (CGT). The authors acknowledge the help from the members of the surface engineering group at McGill and the R&D team at CGT.

REFERENCES

1. Christie, R. M., Pigments for plastics. In *Plastics Additives: An A-Z reference*, Pritchard, G., Ed. Springer Netherlands: Dordrecht, 1998; pp 485-498.
2. Hao, J.; Mohamad, R.; Mahssa, A.; Bozena, K., Solvent-free optical recording of structural colours on pre-imprinted photocrosslinkable nanostructures. *Nano Futures* **2017,** *1* (2), 025001.
3. Yousif, E.; Hasan, A., Photostabilization of poly(vinyl chloride) – Still on the run. *Journal of Taibah University for Science* **2015,** *9* (4), 421-448.
4. Rebollar, E.; Castillejo, M.; Ezquerra, T. A., Laser induced periodic surface structures on polymer films: From fundamentals to applications. *Eur. Polym. J.* **2015,** *73*, 162-174.
5. Ahmmed, K. M. T.; Grambow, C.; Kietzig, A.-M., Fabrication of Micro/Nano Structures on Metals by Femtosecond Laser Micromachining. *Micromachines* **2014,** *5* (4), 1219-1253.
6. Tan, D. Z.; Sharafudeen, K. N.; Yue, Y. Z.; Qiu, J. R., Femtosecond laser induced phenomena in transparent solid materials: Fundamentals and applications. *Prog. Mater Sci.* **2016,** *76*, 154-228.
7. Toosi, S. F.; Moradi, S.; Hatzikiriakos, S. G., Fabrication of Micro/Nano Patterns on Polymeric Substrates Using Laser Ablation Methods to Control Wettability Behaviour: A Critical Review. *Rev. Adhes. Adhes.* **2017,** *5* (1), 55-78.
8. Vorobyev, A. Y.; Guoa, C. L., Colorizing metals with femtosecond laser pulses. *Appl. Phys. Lett.* **2008,** *92* (4), 041914.
9. Khafaji, N. Y.; Demir, A. G.; Vitali, L.; Fustinoni, D.; Niro, A.; Previtali, B.; Taha, Z. A., Optical characterization of laser coloured titanium under different processing atmospheres. *Surf. Coat. Technol.* **2017,** *321*, 156-163.
10. Samad, R. E.; Courrol, L. C.; Lugao, A. B.; de Freitas, A. Z.; Vieira, N. D., Production of color centers in PMMA by ultrashort laser pulses. *Radiat. Phys. Chem.* **2010,** *79* (3), 355-357.
11. Okoshi, M.; Inoue, N., Laser ablation of polymers using 395 nm and 790 nm femtosecond lasers. *Appl. Phys. A* **2004,** *79* (4-6), 841-844.
12. Nouh, S. A.; Benthami, K.; Abutalib, M. M., Modification of structural and optical properties of polyvinyl alcohol/polyethylene glycol thin film by laser irradiation. *Radiat Eff. Defects Solids* **2016,** *171* (1-2), 87-95.
13. Lippert, T.; Dickinson, J. T., Chemical and spectroscopic aspects of polymer ablation: Special features and novel directions. *Chem. Rev.* **2003,** *103* (2), 453-485.
14. Yu, J.; Sun, L.; Ma, C.; Qiao, Y.; Yao, H., Thermal degradation of PVC: A review. *Waste Manage. (Oxford)* **2016,** *48*, 300-314.
15. Bityurin, N., 8 Studies on laser ablation of polymers. *Annual Reports Section "C" (Physical Chemistry)* **2005,** *101* (0), 216-247.
16. Shirk, M. D.; Molian, P. A., A review of ultrashort pulsed laser ablation of materials. *J. Laser Appl.* **1998,** *10* (1), 18-28.
17. Ahmmed, K. M. T.; Ling, E. J. Y.; Servio, P.; Kietzig, A. M., Introducing a new optimization tool for femtosecond laser-induced surface texturing on titanium, stainless steel, aluminum and copper. *Opt. Lasers Eng.* **2015,** *66*, 258-268.
18. Liu, J. M., Simple technique for measurements of pulsed Gaussian-beam spot sizes. *Opt. Lett.* **1982,** *7* (5), 196-198.
19. Mannion, P. T.; Magee, J.; Coyne, E.; O'Connor, G. M.; Glynn, T. J., The effect of damage accumulation behaviour on ablation thresholds and damage morphology in ultrafast laser micro-machining of common metals in air. *Appl. Surf. Sci.* **2004,** *233* (1-4), 275-287.
20. Sun, Z.; Lenzner, M.; Rudolph, W., Generic incubation law for laser damage and ablation thresholds. *J. Appl. Phys.* **2015,** *117* (7), 073102.

21. Rebollar, E.; de Aldana, J. R. V.; Perez-Hernandez, J. A.; Ezquerra, T. A.; Moreno, P.; Castillejo, M., Ultraviolet and infrared femtosecond laser induced periodic surface structures on thin polymer films. *Appl. Phys. Lett.* **2012,** *100* (4).
22. Assaf, Y.; Kietzig, A.-M., Optical and chemical effects governing femtosecond laser-induced structure formation on polymer surfaces. *Materials Today Communications* **2018,** *14*, 169-179.
23. Kruger, J.; Kautek, W., Ultrashort pulse laser interaction with dielectrics and polymers. *Adv. Polym. Sci.* **2004,** *168*, 247-289.
24. Stromberg, R. R.; Straus, S.; Achhammer, B. G., Infrared Spectra of Thermally Degraded Poly(Vinyl-Chloride). *J Res Nat Bur Stand* **1958,** *60* (2), 147-152.
25. Lampman, S., *Characterization and Failure Analysis of Plastics*. ASM International: 2003.
26. Walzak, M. J.; Davidson, R.; Biesinger, M., The use of XPS, FTIR, SEM/EDX, contact angle, and AFM in the characterization of coatings. *J. Mater. Eng. Perform.* **1998,** *7* (3), 317-323.
27. Blazevska-Gilev, J.; Kupčík, J.; Šubrt, J.; Bastl, Z.; Vorlíček, V.; Galíková, A.; Spaseska, D.; Pola, J., IR laser ablation of poly(vinyl chloride): Formation of monomer and deposition of nanofibres of chlorinated polyhydrocarbon. *Polym. Degrad. Stab.* **2006,** *91* (2), 213-220.
28. Rabek, J. F.; Rånby, B.; Östensson, B.; Flodin, P., Oxidation of polyene structures in poly(vinyl chloride) by molecular oxygen and singlet oxygen. *J. Appl. Polym. Sci.* **1979,** *24* (12), 2407-2413.
29. Wypych, G., Degradation by other forms of radiation. In *PVC Degradation and Stabilization (Third Edition)*, ChemTec Publishing: Boston, 2015; pp 215-226.
30. Kupčík, J.; Blazevska-Gilev, J.; Pola, J., IR Laser-Induced Degradation of Poly(vinyl acetate): Novel Thermal Reactions in Solid Polymers. *Macromol. Rapid Commun.* **2005,** *26* (5), 386-389.